

Article

**Crystal Structure and Nontypical Deep-
Red Luminescence of $\text{Ca}_3\text{Mg}[\text{Li}_2\text{Si}_2\text{N}_6]:\text{Eu}^{2+}$**

Christine Poesl, and Wolfgang Schnick

Chem. Mater., **Just Accepted Manuscript** • DOI: 10.1021/acs.chemmater.7b00871 • Publication Date (Web): 03 Apr 2017Downloaded from <http://pubs.acs.org> on April 4, 2017**Just Accepted**

"Just Accepted" manuscripts have been peer-reviewed and accepted for publication. They are posted online prior to technical editing, formatting for publication and author proofing. The American Chemical Society provides "Just Accepted" as a free service to the research community to expedite the dissemination of scientific material as soon as possible after acceptance. "Just Accepted" manuscripts appear in full in PDF format accompanied by an HTML abstract. "Just Accepted" manuscripts have been fully peer reviewed, but should not be considered the official version of record. They are accessible to all readers and citable by the Digital Object Identifier (DOI®). "Just Accepted" is an optional service offered to authors. Therefore, the "Just Accepted" Web site may not include all articles that will be published in the journal. After a manuscript is technically edited and formatted, it will be removed from the "Just Accepted" Web site and published as an ASAP article. Note that technical editing may introduce minor changes to the manuscript text and/or graphics which could affect content, and all legal disclaimers and ethical guidelines that apply to the journal pertain. ACS cannot be held responsible for errors or consequences arising from the use of information contained in these "Just Accepted" manuscripts.

**ACS Publications**

Crystal Structure and Nontypical Deep-Red Luminescence of $\text{Ca}_3\text{Mg}[\text{Li}_2\text{Si}_2\text{N}_6]:\text{Eu}^{2+}$

Christine Poesl and Wolfgang Schnick*

Department of Chemistry, University of Munich (LMU), Butenandtstr. 5-13 (D), 81377 Munich, Germany

ABSTRACT: Rare-earth doped nitridosilicates exhibit outstanding luminescence properties and have been intensively studied for solid-state lighting. Here, we describe the new nitridolithosilicate $\text{Ca}_3\text{Mg}[\text{Li}_2\text{Si}_2\text{N}_6]:\text{Eu}^{2+}$ with extraordinary luminescence characteristics. The compound was synthesized by solid-state metathesis reaction in sealed Ta ampules. The crystal structure was solved and refined on the basis of single-crystal X-ray diffraction data. $\text{Ca}_3\text{Mg}[\text{Li}_2\text{Si}_2\text{N}_6]:\text{Eu}^{2+}$ crystallizes in the monoclinic space group $C2/m$ (no. 12) [$Z = 4$, $a = 5.966(1)$, $b = 9.806(2)$, $c = 11.721(2)$ Å, $\beta = 99.67(3)^\circ$, $V = 675.9(2)$ Å³] and exhibits a layered anionic network made up of edge- and corner-sharing LiN_4 tetrahedra and $[\text{Si}_2\text{N}_6]^{10-}$ bow-tie units. The network charge is compensated by Ca^{2+} and Mg^{2+} ions. Upon irradiation with UV to blue light, red emission at exceptionally long wavelengths ($\lambda_{\text{em}} = 734$ nm, $\text{fwhm} \approx 2293$ cm⁻¹) is observed. According to emission in the near infrared, application in LEDs for horticultural lighting appears promising.

INTRODUCTION

Nitridosilicates are characterized by its manifold structural chemistry and intriguing materials properties. Due to the high sensitivity to air and moisture of both starting materials and products, synthesis of less condensed nitridosilicates is quite challenging. Over the last years, different synthetic approaches leading to nitridosilicates have been elaborated. These include high-temperature reactions, precursor routes, ammonothermal syntheses and flux methods by using, for example, liquid sodium.¹⁻⁹ Solid-state metathesis reactions have gained significant importance as well, since a variety of ternary or higher nitrides have recently been synthesized by this approach.¹⁰⁻¹⁵ Thereby, key feature is the employment of reactive starting materials by coproducing a metathesis salt, which on one hand drives the reaction thermodynamically and on the other hand concurrently acts as reactive flux.

Common structural motifs of nitridosilicates are SiN_4 tetrahedra, which may be linked through vertices and/or edges, forming more or less condensed anionic substructures ranging up to three-periodic anionic frameworks. The resulting structural diversity of nitridosilicates can be ascribed to the N atoms, which are able to connect up to four adjacent tetrahedral centers. Cations like alkaline earths (AE^{2+}), Li^+ or Mg^{2+} are distributed among the voids of the anionic networks and balance their charges. As some examples in literature have already shown, the number of new nitrides can be further increased by partial substitution of Si^{4+} by Li^+ , Mg^{2+} or Al^{3+} .^{12-13,16-19} Complete exchange of Si^{4+} by Ga^{3+} or Ge^{4+} is also possible and results in the strongly related compound classes of nitridogallates and nitridogermanates, respectively (see homeotypical

compounds $\text{Ba}[\text{Mg}_3\text{SiN}_4]$, $\text{Sr}[\text{Mg}_3\text{GeN}_4]$, and $M[\text{Mg}_2\text{Ga}_2\text{N}_4]$ with $M = \text{Sr}, \text{Ba}$).^{17,20-21}

Nitridosilicates show a great diversity of interesting materials properties, e.g. high mechanical strength and high thermal stability of silicon nitride ceramics, lithium ion conductivity (e.g. Li_2SiN_2)²²⁻²³ or luminescence when doped with Eu^{2+} or Ce^{3+} .^{22,24-28} $(\text{Sr}, \text{Ba})_2\text{Si}_5\text{N}_8:\text{Eu}^{2+}$,²⁹⁻³¹ $\text{CaAlSiN}_3:\text{Eu}^{2+}$,⁹ and $\text{SrMg}_3\text{SiN}_4:\text{Eu}^{2+}$ ¹⁶ represent prominent examples of rare-earth doped nitrides, which show strong broadband emission in the red spectral region after irradiation with blue light, originating from parity allowed $4f^65d^1 \rightarrow 4f^7$ transitions in Eu^{2+} and spin and parity allowed $4f^65d^1 \rightarrow 4f^7$ transitions in Ce^{3+} . Warm white light can be generated by combination of red and green emitting phosphors, both covered on a blue LED chip, which is usually an (In,Ga)N semiconductor chip.³²⁻³³ The so-called phosphor-converted light-emitting diodes (pc-LEDs) are highly efficient and, over the last decade, developed into an energy-saving replacement for inefficient incandescent light bulbs. Since most commercially available warm white pc-LEDs still show a large portion of its emission beyond the sensitivity of the human eye,³⁴⁻³⁵ research for narrow-band red emitting luminescent materials is of particular interest for general illumination purposes.

During our research for innovative red emitting compounds, we came across $\text{Ca}_3\text{Mg}[\text{Li}_2\text{Si}_2\text{N}_6]:\text{Eu}^{2+}$, a new nitridolithosilicate with outstanding emission properties at fairly long wavelengths. In this contribution, we report on synthesis, structural elucidation, and optical properties of $\text{Ca}_3\text{Mg}[\text{Li}_2\text{Si}_2\text{N}_6]:\text{Eu}^{2+}$. Unprecedented luminescence properties differ essentially from previously described Eu^{2+} -doped nitridosilicates and are discussed in detail, also in

comparison to recently reported narrow-band red emitting Eu^{2+} -doped nitridosilicates.

EXPERIMENTAL SECTION

Synthesis. Due to the sensitivity of the starting materials and the product towards air and moisture, all manipulations were performed under inert-gas conditions using argon filled glove boxes (Unilab, MBraun, Garching, $\text{O}_2 < 1$ ppm, $\text{H}_2\text{O} < 1$ ppm) and combined Schlenk/vacuum lines. Ar was dried and purified by passing through glass tubes filled with silica gel (Merck), molecular sieve (Fluka, 4 Å), P_4O_{10} (Roth, $\geq 99\%$) and titanium sponge (Johnsen Matthey, 99.5%). $\text{Ca}_3\text{Mg}[\text{Li}_2\text{Si}_2\text{N}_6]:\text{Eu}^{2+}$ was synthesized by solid-state metathesis reaction using $\text{Ca}(\text{NH}_2)_2$ (17.9 mg, 0.25 mmol, synthesized according to Brokamp),³⁶ CaH_2 (8.3 mg, 0.20 mmol, Cerac, 99.5%), MgF_2 (15.5 mg, 0.25 mmol, ABCR, 99.99%), Si_3N_4 (6.9 mg, 0.05 mmol, UBE, 99.9%), 1.7 mol% EuF_3 (0.9 mg, $4.3 \cdot 10^{-3}$ mmol, Sigma-Aldrich, 99.99%), and Li (9.8 mg, 1.41 mmol, Alfa Aesar, 99.9%) as starting materials. The powdery reactants were finely ground and placed with metallic Li in a tantalum ampule, which was weld shut in an arc furnace. The reaction mixture was heated up to 950 °C with a rate of 300 °C·h⁻¹, maintained for 24 h, subsequently cooled down to 500 °C with a rate of 5 °C·h⁻¹ and finally quenched to room temperature by switching off the furnace. Orange colored single crystals of $\text{Ca}_3\text{Mg}[\text{Li}_2\text{Si}_2\text{N}_6]:\text{Eu}^{2+}$ were obtained embedded in an amorphous powder. Additionally, red rod-shaped crystals of $\text{Ca}[\text{Mg}_3\text{SiN}_4]:\text{Eu}^{2+}$, colorless crystals of LiF, and some metallic residues were found as side phases of the reaction. The sample is sensitive towards air and moisture and partially shows intensive red luminescence under irradiation with ultraviolet (UV) to green light.

Single-Crystal X-ray Diffraction. Single crystals of $\text{Ca}_3\text{Mg}[\text{Li}_2\text{Si}_2\text{N}_6]:\text{Eu}^{2+}$ were isolated from the reaction product, washed with dry paraffin oil and enclosed in glass capillaries, which were sealed under argon to avoid hydrolysis. X-ray diffraction data were collected on a Stoe IPDS I diffractometer (Mo- K_α radiation, graphite monochromator). Structure solution was done in SHELXS-97,³⁷ by using direct methods. The crystal structure was refined by full-matrix least-squares calculation on $|F|^2$ in SHELXL-97³⁸⁻³⁹ with anisotropic displacement parameters for all atoms. Further details of the crystal-structure refinement may be obtained from the Fachinformationszentrum Karlsruhe, 76344 Eggenstein-Leopoldshafen, Germany (Fax: +49-7247-808-666; E-mail: crysdata@fiz-karlsruhe.de), on quoting the depository number CSD-432605.

Scanning Electron Microscopy. The chemical composition of $\text{Ca}_3\text{Mg}[\text{Li}_2\text{Si}_2\text{N}_6]:\text{Eu}^{2+}$ was confirmed by energy dispersive X-ray spectroscopy (FEI Helios G3 UC scanning electron microscope equipped with an EDX detector, scanning transmission detector and focused ion beam). The reaction product was placed on an adhesive conductive carbon pad and coated with a conductive carbon film (BAL-TEC MED 020, Bal Tec AG).

Luminescence. Luminescence investigations on single crystals of $\text{Ca}_3\text{Mg}[\text{Li}_2\text{Si}_2\text{N}_6]:\text{Eu}^{2+}$ were performed using a luminescence microscope, consisting of a HORIBA Fluorimax4 Spectrofluorimeter system, which is attached to an Olympus BX51 microscope via fiber optics. The single crystals were measured in sealed glass capillaries with an excitation wavelength of 440 nm. The emission spectrum was measured between 460 and 800 nm; the excitation spectrum was measured between 380 and 680 nm, with a step size of 2 nm, respectively. Since $\text{Ca}_3\text{Mg}[\text{Li}_2\text{Si}_2\text{N}_6]:\text{Eu}^{2+}$ shows emission beyond 800 nm and the spectrometer is only calibrated for wavelengths up to 800 nm, emission peak in the near infrared was simulated using a Gauss-fit.

RESULTS AND DISCUSSION

Synthesis and Chemical Analysis. Solid-state metathesis reaction as described above yielded a heterogeneous reaction mixture containing single-crystals of $\text{Ca}_3\text{Mg}[\text{Li}_2\text{Si}_2\text{N}_6]:\text{Eu}^{2+}$. The crystals show orange body color and undergo rapid hydrolysis when exposed to air. The elemental composition was determined by energy-dispersive X-ray spectroscopy (EDX). Due to the method, light elements like N cannot be determined with a reasonable degree of accuracy, also Li is not determinable. The atomic ratio Ca/Mg/Si of 3.0/1.1/2.0 (six measurements on different crystals), normalized to the Ca content, is in good agreement with the sum formula obtained from single-crystal structure analysis. Besides a small amount of oxygen, which can be attributed to superficial hydrolysis of the product, no further elements were detected.

Single-Crystal Structure Analysis. The crystal structure of $\text{Ca}_3\text{Mg}[\text{Li}_2\text{Si}_2\text{N}_6]:\text{Eu}^{2+}$ was solved and refined in the monoclinic space group $C2/m$ (no. 12) with $a = 5.966(1)$, $b = 9.806(2)$, $c = 11.721(2)$ Å, and $\beta = 99.67(3)^\circ$. The crystallographic data are summarized in Table 1. Atomic coordinates, Wyckoff positions, and isotropic displacement parameters are listed in Table 2. Selected bond lengths and angles as well as anisotropic displacement parameters are given in the Supporting Information (Tables Si-S3). Due to the small dopant concentration and, therefore, the insignificant scattering intensity, Eu^{2+} was neglected during structure refinement.

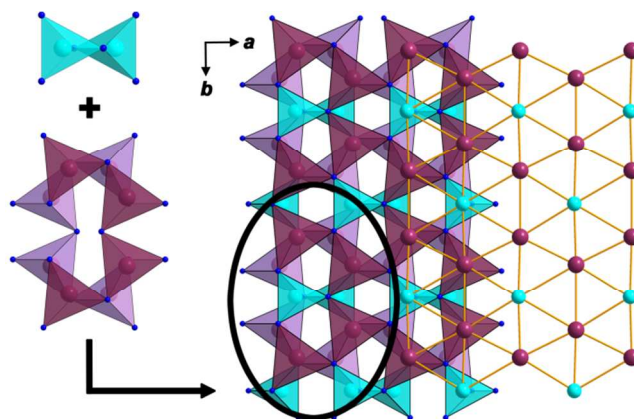


Figure 1. Details of layers in $\text{Ca}_3\text{Mg}[\text{Li}_2\text{Si}_2\text{N}_6]:\text{Eu}^{2+}$. Left: $[\text{Si}_2\text{N}_6]^{10-}$ bow-tie units (turquoise) and *achter* rings of LiN_4 tetrahedra (violet). Right: Layer made up of bow-tie units and *achter* rings forming two sublayers of condensed *dreier* rings, only one of them shown for reasons of clarity.

The crystal structure of $\text{Ca}_3\text{Mg}[\text{Li}_2\text{Si}_2\text{N}_6]:\text{Eu}^{2+}$ is closely related to that of $\text{Ca}_2\text{Mg}[\text{Li}_4\text{Si}_2\text{N}_6]$,¹² which has already been reported in literature. Both structures contain identical layers of LiN_4 and SiN_4 tetrahedra as well as Ca and Mg ions, which are located between the layers. Since Li as well as Si are part of the tetrahedral network, the compounds can be more precisely classified as nitridolithosilicates. The arrangement of tetrahedra within one layer is shown in Figure 1. It consists of vertex- and corner-sharing LiN_4 tetrahedra forming *achter* rings,⁴⁰ intercalated by edge-sharing $[\text{Si}_2\text{N}_6]^{10-}$ “bow-tie” units. This results in layers of condensed *dreier* rings in the *ab* plane. The differences between the structurally related compounds $\text{Ca}_2\text{Mg}[\text{Li}_4\text{Si}_2\text{N}_6]$ and $\text{Ca}_3\text{Mg}[\text{Li}_2\text{Si}_2\text{N}_6]:\text{Eu}^{2+}$ are additional $[\text{Si}_2\text{N}_6]^{10-}$ bow-tie units in the crystal structure of $\text{Ca}_3\text{Mg}[\text{Li}_2\text{Si}_2\text{N}_6]:\text{Eu}^{2+}$. Together with the Ca^{2+} and Mg^{2+} ions, these bow-tie units are located between layers of *dreier* rings. A direct comparison of both crystal structures is illustrated in Figure 2.

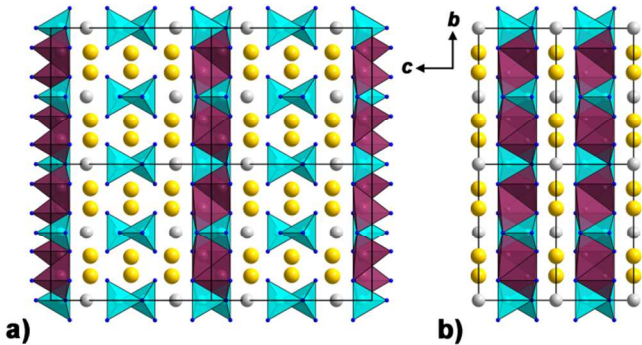


Figure 2. Crystal structures of $\text{Ca}_3\text{Mg}[\text{Li}_2\text{Si}_2\text{N}_6]:\text{Eu}^{2+}$ (a) and $\text{Ca}_2\text{Mg}[\text{Li}_4\text{Si}_2\text{N}_6]$ (b).

$[\text{Si}_2\text{N}_6]^{10-}$ bow-tie units were first described in $\text{Ba}_5\text{Si}_2\text{N}_6$,² and are also known in other nitridosilicates, e.g. $\text{Ca}_2\text{Mg}[\text{Li}_4\text{Si}_2\text{N}_6]$, $\text{Li}_2\text{Ca}_2[\text{Mg}_2\text{Si}_2\text{N}_6]$,¹² and $\text{Ca}_3[\text{Li}_4\text{Si}_2\text{N}_6]$.⁴¹⁻⁴² Si–N bond lengths in these bow-tie units ($\text{Ca}_3\text{Mg}[\text{Li}_2\text{Si}_2\text{N}_6]:\text{Eu}^{2+}$: 1.719(5)–1.843(7) Å) are slightly larger than distances found in other nitridosilicates.^{1,5,16,43-44} This can be attributed to the repulsion of the Si atoms in the pairs of edge-sharing SiN_4 tetrahedra (Si–Si: 2.363(4)–2.477(4) Å), which in turn is related to a reduced angle N–Si–N. Li–N distances range from 2.088(11) to 2.225(11) Å and are in good agreement with distances known from other nitrides and with the sum of the ionic radii.^{11,44-46}

Ca^{2+} and Mg^{2+} ions balance the charges of the anionic framework. Its coordination spheres are displayed in Figure 3. Ca^{2+} occupies two different sites with distorted oc-

tahedral coordination by N and with distances varying from 2.310(4)–2.744(5) Å. Mg^{2+} exhibits fourfold rectangular surroundings by N. Mg–N bond lengths are in a range of 2.159(5)–2.199(5) Å. Additionally, there is one further N atom at a distance of 2.693(7) Å, its coordination to Mg1 is illustrated in Figure 3 by a dashed line. Ca–N as well as Mg–N distances correspond to the sums of the ionic radii (2.55 and 2.10 Å, respectively)⁴⁵ as well as to distances known from other nitridosilicates.^{1,12,16} The Madelung part of the lattice energy has been calculated to confirm the crystal structure of $\text{Ca}_3\text{Mg}[\text{Li}_2\text{Si}_2\text{N}_6]:\text{Eu}^{2+}$.^{45,47-49} Therefore, the charge, distance, and coordination spheres of constituting ions were taken into account. MAPLE values for $\text{Ca}_3\text{Mg}[\text{Li}_2\text{Si}_2\text{N}_6]:\text{Eu}^{2+}$ and its constituting binary and ternary nitrides are given in Table 3. The resulting deviation of 0.31% verifies the electrostatic consistency of the refined structure.

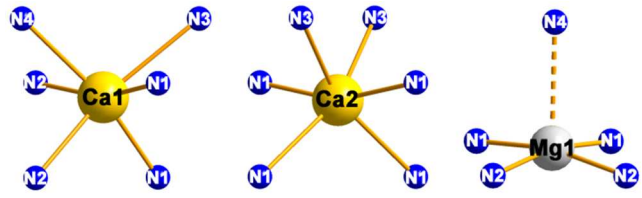


Figure 3. Coordination spheres of counter ions Ca^{2+} and Mg^{2+} .

Table 1. Crystallographic data of the single-crystal structure determination of $\text{Ca}_3\text{Mg}[\text{Li}_2\text{Si}_2\text{N}_6]:\text{Eu}^{2+}$.

formula	$\text{Ca}_3\text{Mg}[\text{Li}_2\text{Si}_2\text{N}_6]:\text{Eu}^{2+}$
crystal system	monoclinic
space group	$C2/m$ (no. 12)
lattice parameters / Å,°	$a = 5.966(1)$ $b = 9.806(2)$ $c = 11.721(2)$ $\beta = 99.67(3)$
cell volume / Å ³	675.9(2)
formula units / unit cell	4
density / g·cm ^{−3}	2.935
μ / mm ^{−1}	2.827
T / K	293(2)
diffractometer	Stoe IPDS I
radiation	Mo- K_α ($\lambda = 0.71073$ Å), graphite monochromator
F(000)	592
profile range	$4.04 \leq \theta \leq 29.90$
index ranges	$-8 \leq h \leq 8$ $-13 \leq k \leq 13$ $-16 \leq l \leq 16$
independent reflections	1028 [$R(\text{int}) = 0.0722$]
refined parameters	72
Goodness of fit	1.323

R_1 (all data); R_1 ($F^2 > 2\sigma(F^2)$)	0.0770, 0.0618
wR_2 (all data); wR_2 ($F^2 > 2\sigma(F^2)$)	0.1118, 0.1080
$\Delta\rho_{\max}, \Delta\rho_{\min}$ / $e\cdot\text{\AA}^{-3}$	0.826, -1.176

Table 2. Atomic coordinates, Wyckoff positions and equivalent isotropic displacement parameters of $\text{Ca}_3\text{Mg}[\text{Li}_2\text{Si}_2\text{N}_6]:\text{Eu}^{2+}$.

atom	Wyck.	x	y	z	$U_{\text{eq}}/\text{\AA}^2$
Ca1	8j	0.0500(2)	0.32384(11)	0.24678(9)	0.0068(2)
Ca2	4h	0	0.1840(2)	1/2	0.0085(3)
Si1	4i	0.3521(3)	0	0.4192(2)	0.0050(4)
Si2	4i	0.6885(3)	0	0.0632(2)	0.0048(4)
Mg1	4i	0.0623(5)	0	0.2220(2)	0.0094(5)
Li1	8j	0.1731(18)	0.1767(11)	0.0594(8)	0.015(2)
N1	8j	0.2335(7)	0.1447(4)	0.3513(4)	0.0070(8)
N2	8j	0.3413(7)	0.3566(5)	0.1179(4)	0.0064(8)
N3	4i	0.3418(10)	0	0.5703(5)	0.0084(12)
N4	4i	0.3943(11)	0	0.0921(5)	0.0068(11)

Table 3. MAPLE values and MAPLE sums / $\text{kJ}\cdot\text{mol}^{-1}$ for $\text{Ca}_3\text{Mg}[\text{Li}_2\text{Si}_2\text{N}_6]:\text{Eu}^{2+}$. Δ is the deviation between the MAPLE sum of $\text{Ca}_3\text{Mg}[\text{Li}_2\text{Si}_2\text{N}_6]:\text{Eu}^{2+}$ and the MAPLE sum of constituting binary and ternary nitrides.^[a]

atom	MAPLE	atom	MAPLE	Σ, Δ
Ca^{2+}	2083	Li^{+}	717	
Ca^{2+}	1812	N^{3-}	5056	
Si^{4+}	9201	N^{2-}	4951	
Si^{4+}	9202	N^{3-}	5440	$\Sigma = 58949$
Mg^{2+}	2241	N^{4-}	5439	$\Delta = 0.31\%$
Total MAPLE: $\text{Ca}_3\text{Mg}[\text{Li}_2\text{Si}_2\text{N}_6] = \text{Ca}_3\text{N}_2 + \frac{1}{3}\text{Mg}_3\text{N}_2 + \frac{2}{3}\text{Li}_2\text{SiN}_2 + \frac{2}{3}\text{LiSi}_2\text{N}_3 = 59131 \text{ kJ}\cdot\text{mol}^{-1}$				

[a] Typical partial MAPLE values / $\text{kJ}\cdot\text{mol}^{-1}$: Ca^{2+} : 1700–2200; Mg^{2+} : 2100–2500; Li^{+} : 550–860; Si^{4+} : 9000–10200; N^{3-} : 4300–6200.^{9,16,50–51}

Luminescence. Addition of EuF_3 to the starting materials yielded a gray microcrystalline sample containing orange colored crystals of $\text{Ca}_3\text{Mg}[\text{Li}_2\text{Si}_2\text{N}_6]:\text{Eu}^{2+}$. Under blue irradiation, the sample shows luminescence in the red spectral region. Due to inhomogeneity of the sample, luminescence investigations have been performed on single crystals of $\text{Ca}_3\text{Mg}[\text{Li}_2\text{Si}_2\text{N}_6]:\text{Eu}^{2+}$ in sealed silica glass capillaries. All crystals show comparable red emission under blue irradiation. Excitation of the title compound with a nominal dopant concentration of 1.7 mol% at 440 nm yields an emission band with a maximum at 734 nm and a full width at half maximum (fwhm) of 2293 cm^{-1} (124 nm). The

Eu^{2+} -doped compound exhibits a maximum absorption around 450 nm and is therefore efficiently excitable with UV to blue light, as provided, for example, by (In,Ga)N-LEDs. Excitation and emission spectra are illustrated in Figure 4.

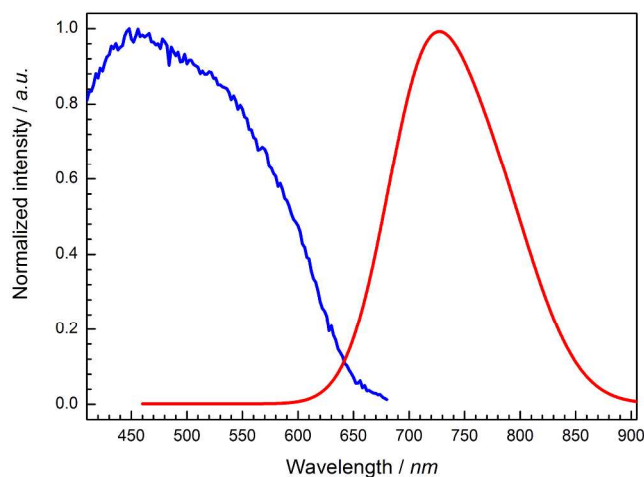


Figure 4. Excitation (blue) and emission (red) spectra of $\text{Ca}_3\text{Mg}[\text{Li}_2\text{Si}_2\text{N}_6]:\text{Eu}^{2+}$.

The broad emission band of $\text{Ca}_3\text{Mg}[\text{Li}_2\text{Si}_2\text{N}_6]:\text{Eu}^{2+}$ is assigned to parity allowed $4f^65d^1 \rightarrow 4f^7$ transitions in Eu^{2+} .^{33,52–53} Since Eu^{2+} is expected to occupy the Ca site, we assume that luminescence originates from octahedrally coordinated Eu^{2+} ions. The presence of two crystallographically different Ca sites with slightly differing distortion of the octahedra and, therefore, different interatomic distances, influences the width of the emission band by broadening. A comparable 6-fold coordination can also be found in $\text{Ba}_3\text{Si}_6\text{O}_{12}\text{N}_2$ ⁵⁴ and its solid-solution series $\text{Ba}_{1-x}\text{Sr}_x\text{Si}_6\text{O}_{12}\text{N}_2$ with $x \approx 0.4$ and 1. These compounds doped with 2 mol% Eu^{2+} exhibit broad emission bands with maxima between 523 and 549 nm (green luminescence) when irradiated with near-UV to blue light. In general, both the spectral position and the band width of the emission strongly depend on the energy level of 5d states of the activator ion, which in turn is influenced by the host lattice. The stronger the covalent interactions between Eu^{2+} and its surroundings, the smaller is the transition energy between 4f and 5d orbitals of the activator ion (nephelauxetic effect). For this reason and because of the higher formal charge of N^{3-} compared to O^{2-} , the 5d states of Eu^{2+} in $\text{Ca}_3\text{Mg}[\text{Li}_2\text{Si}_2\text{N}_6]:\text{Eu}^{2+}$ are at lower energies than those in $\text{Ba}_3\text{Si}_6\text{O}_{12}\text{N}_2:\text{Eu}^{2+}$ and $\text{Ba}_{1-x}\text{Sr}_x\text{Si}_6\text{O}_{12}\text{N}_2:\text{Eu}^{2+}$, respectively, and emission of $\text{Ca}_3\text{Mg}[\text{Li}_2\text{Si}_2\text{N}_6]:\text{Eu}^{2+}$ occurs at longer wavelengths.

Typical Eu^{2+} emission of other compound classes are in a range of 356–461 nm (fluorides), 360–540 nm (oxosilicates), 420–555 nm (aluminates and gallates), 470–660 nm (sulfides) and 529–670 nm (nitrides).^{55–56} The here presented nitridolithosilicate $\text{Ca}_3\text{Mg}[\text{Li}_2\text{Si}_2\text{N}_6]:\text{Eu}^{2+}$ is, to the best of our knowledge and except for $\text{CaO}:\text{Eu}^{2+}$ ($\lambda_{\text{em}} = 733 \text{ nm}$),^{57–58} and $\text{MH}_2:\text{Eu}^{2+}$ ($M = \text{Ca}, \text{Sr}, \text{Ba}$; $\lambda_{\text{em}} = 728\text{--}764 \text{ nm}$)⁵⁹ the first and so far the only example of a Eu^{2+} -

doped compound that emits at fairly long wavelengths of >700 nm.

Recently, we reported on luminescence investigations of the nitridomagnesosilicate $\text{Li}_2(\text{Ca}_{1-x}\text{Sr}_x)_2[\text{Mg}_2\text{Si}_2\text{N}_6]:\text{Eu}^{2+}$ ($x = 0$ and 0.6),⁶⁰ with a nominal dopant concentration of 1 mol%. Just as $\text{Ca}_3\text{Mg}[\text{Li}_2\text{Si}_2\text{N}_6]:\text{Eu}^{2+}$, the crystal structure of $\text{Li}_2(\text{Ca}_{1-x}\text{Sr}_x)_2[\text{Mg}_2\text{Si}_2\text{N}_6]:\text{Eu}^{2+}$ contains $[\text{Si}_2\text{N}_6]^{10-}$ bow-tie units. In contrast to the here presented nitridolithosilicate with LiN_4 and SiN_4 tetrahedra as network-building structural motifs and Ca^{2+} and Mg^{2+} as counter ions, Li^+ and Ca^{2+} compensate the negative charge of the network, which, in $\text{Li}_2(\text{Ca}_{1-x}\text{Sr}_x)_2[\text{Mg}_2\text{Si}_2\text{N}_6]:\text{Eu}^{2+}$, is made up of MgN_4 and SiN_4 tetrahedra. In the latter compound, chains of edge-sharing MgN_4 tetrahedra are interconnected by bow-tie units, forming *vierer* and *sechser* ring channels along $[100]$. Whereas Li^+ ions are located within *vierer* ring channels, Ca^{2+} (Sr^{2+}) ions and, therefore, also Eu^{2+} ions, show distorted octahedral coordination by N within *sechser* ring channels. When irradiated with blue light, narrow-band red emission also occurs at rather long wavelengths of 638 nm ($x = 0$) and 634 nm ($x = 0.6$) with $\text{fwhm} = 1513\text{--}1532$ cm^{-1} , respectively.

Both $\text{Li}_2(\text{Ca}_{1-x}\text{Sr}_x)_2[\text{Mg}_2\text{Si}_2\text{N}_6]:\text{Eu}^{2+}$ and $\text{Ca}_3\text{Mg}[\text{Li}_2\text{Si}_2\text{N}_6]:\text{Eu}^{2+}$ exhibit similar body colors and show similarities in their absorption bands. The main difference between both nitridosilicates is the Stokes shift, which is larger for $\text{Ca}_3\text{Mg}[\text{Li}_2\text{Si}_2\text{N}_6]:\text{Eu}^{2+}$. This can be attributed to differences in the chemical surroundings of Eu^{2+} , which in each case is expected to occupy the Ca^{2+} (Sr^{2+}) site, and also to differences in the phonon frequencies of respective host lattices. $\text{Li}_2(\text{Ca}_{1-x}\text{Sr}_x)_2[\text{Mg}_2\text{Si}_2\text{N}_6]:\text{Eu}^{2+}$ exhibits only one crystallographic Ca site (Wyckoff position $4g$ of space group C_2/m) with three different Ca–N distances between 2.49 and 2.75 Å. In $\text{Ca}_3\text{Mg}[\text{Li}_2\text{Si}_2\text{N}_6]:\text{Eu}^{2+}$, nine interatomic distances Ca–N of two Ca sites (Wyckoff positions $8j$ and $4h$ of space group C_2/m) vary between 2.31 and 2.74 Å. This is, in comparison, a significantly larger spread and entails chemical differentiation of both sites, which eventually leads to a composed emission band of Eu^{2+} on either of the crystallographic sites. Moreover, the shorter bond lengths Ca–N in $\text{Ca}_3\text{Mg}[\text{Li}_2\text{Si}_2\text{N}_6]:\text{Eu}^{2+}$, especially occurring on the lowest symmetry Ca_1 site, may entail efficient energy transfer from Eu^{2+} incorporated on the larger higher symmetry Ca_2 site and, thus, also lead to a more pronounced red shift of the emission band for the Eu doping concentration investigated in this report. Whereas in $\text{Li}_2(\text{Ca}_{1-x}\text{Sr}_x)_2[\text{Mg}_2\text{Si}_2\text{N}_6]:\text{Eu}^{2+}$, infinite chains of edge-sharing MgN_4 tetrahedra are interconnected by $[\text{Si}_2\text{N}_6]^{10-}$ bow-tie units leading to a three-periodic network, $\text{Ca}_3\text{Mg}[\text{Li}_2\text{Si}_2\text{N}_6]:\text{Eu}^{2+}$ consists of layers made up of LiN_4 and SiN_4 tetrahedra and isolated bow-tie units. Consequently, due to the lower degree of condensation and also due to lower symmetry of the Ca_1 site with its short Ca–N contact lengths, local lattice relaxation of Eu^{2+} in its excited state in $\text{Ca}_3\text{Mg}[\text{Li}_2\text{Si}_2\text{N}_6]:\text{Eu}^{2+}$ is expected to be larger than in $\text{Li}_2(\text{Ca}_{1-x}\text{Sr}_x)_2[\text{Mg}_2\text{Si}_2\text{N}_6]:\text{Eu}^{2+}$,⁶¹ resulting in a larger Stokes shift of the title compound.

Red emission and extremely narrow band widths with $\text{fwhm} < 1200$ cm^{-1} have been reported for $\text{Sr}[\text{Mg}_3\text{SiN}_4]:\text{Eu}^{2+}$

(1170 cm^{-1}), and $\text{Sr}[\text{LiAl}_3\text{N}_4]:\text{Eu}^{2+}$ (1180 cm^{-1}).^{16,34} Both compounds show a highly symmetric cube-like coordination of the alkaline earth ion by N.

CONCLUSION

In this contribution, we report on $\text{Ca}_3\text{Mg}[\text{Li}_2\text{Si}_2\text{N}_6]:\text{Eu}^{2+}$, a new nitridolithosilicate with exceptional luminescence properties. The compound was synthesized by solid-state metathesis reaction and could be obtained as orange colored single crystals within an amorphous powder. The crystal structure of $\text{Ca}_3\text{Mg}[\text{Li}_2\text{Si}_2\text{N}_6]:\text{Eu}^{2+}$ is related to that of $\text{Ca}_2\text{Mg}[\text{Li}_4\text{Si}_2\text{N}_6]$. It consists of corner- and edge-sharing LiN_4 tetrahedra, intercalated by $[\text{Si}_2\text{N}_6]^{10-}$ bow-tie units forming anionic layers, which are separated by isolated $[\text{Si}_2\text{N}_6]^{10-}$ bow-tie units and Ca^{2+} and Mg^{2+} ions. The latter two act as counter ions and compensate the negative charge of the anionic framework. Up to now, only a small number of nitridosilicates containing Li^+ and Mg^{2+} ions are known from literature, namely $\text{Ca}_2\text{Mg}[\text{Li}_4\text{Si}_2\text{N}_6]$, $\text{Li}_2\text{Ca}_2[\text{Mg}_2\text{Si}_2\text{N}_6]$, and $\text{Li}_2(\text{Ca}_{1.86}\text{Sr}_{0.14})[\text{Mg}_2\text{Si}_2\text{N}_6]$.^{12,60} Thereby, Li^+ and Mg^{2+} ions may either be part of the tetrahedral network or act as counter ions. This behavior may significantly increase the variety of possible structures within the class of nitridosilicates.

Recently, the quest for narrow-band red emitting phosphors has been triggered by attempts to improve luminescence properties of commercially available pc-LEDs for general illumination and signaling purposes.^{16,34,62} Meanwhile, LED technology for other specific applications is on the advance and will increasingly be pursued. This includes, for example, LED technology for plants, in order to replace currently used lamps to reduce costs and, seen in the long term, improve productivity by optimizing growth environments.⁶³ Similar to requirements for LEDs applied for general illumination, LEDs with regard to application in horticulture have to be cheap, environmentally friendly, highly efficient and reliable. Luminescence investigations on $\text{Ca}_3\text{Mg}[\text{Li}_2\text{Si}_2\text{N}_6]:\text{Eu}^{2+}$ show red emission peaking at 734 nm and a fwhm of 2293 cm^{-1} (124 nm). This represents an unexpected emission at fairly long wavelengths, not yet known for Eu^{2+} -doped nitrides. Despite emission >700 nm and, therefore, too high energy loss beyond the sensitivity of the human eye when applied in pc-LEDs, $\text{Ca}_3\text{Mg}[\text{Li}_2\text{Si}_2\text{N}_6]:\text{Eu}^{2+}$ may find application in more specialized fields like horticultural lighting.

ASSOCIATED CONTENT

Supporting Information. Selected bond lengths in $\text{Ca}_3\text{Mg}[\text{Li}_2\text{Si}_2\text{N}_6]:\text{Eu}^{2+}$ (Table S1), selected bond angles in $\text{Ca}_3\text{Mg}[\text{Li}_2\text{Si}_2\text{N}_6]:\text{Eu}^{2+}$ (Table S2), and anisotropic displacement parameters for $\text{Ca}_3\text{Mg}[\text{Li}_2\text{Si}_2\text{N}_6]:\text{Eu}^{2+}$ (Table S3). This material is available free of charge via the Internet at <http://pubs.acs.org>.

AUTHOR INFORMATION

Corresponding Author

* E-mail: wolfgang.schnick@uni-muenchen.de

Notes

The authors declare no competing financial interest.

ACKNOWLEDGMENT

The authors thank Philipp Bielec for collecting single-crystal X-ray data as well as Christian Minke (both at Department of Chemistry, University of Munich) for EDX measurements. Our thanks also go to Petra Huppertz (Lumileds Development Center Aachen) for luminescence measurements as well as Volker Weiler and Peter Schmidt (Lumileds Development Center Aachen) for discussions. Financial support from the Fonds der Chemischen Industrie (FCI) is gratefully acknowledged.

REFERENCES

- (1) Gál, Z. A.; Mallinson, P. M.; Orchard, H. J.; Clarke, S. J. Synthesis and Structure of Alkaline Earth Silicon Nitrides: BaSiN_2 , SrSiN_2 , and CaSiN_2 . *Inorg. Chem.* **2004**, *43*, 3998-4006.
- (2) Yamane, H.; DiSalvo, F. J. Preparation and crystal structure of a new barium silicon nitride, $\text{Ba}_5\text{Si}_2\text{N}_6$. *J. Alloys Compd.* **1996**, *240*, 33-36.
- (3) Watanabe, T.; Nonaka, K.; Li, J.; Kishida, K.; Yoshimura, M. Low temperature ammonothermal synthesis of europium-doped SrAlSiN_3 for a nitride red phosphor. *J. Ceram. Soc. Jpn.* **2012**, *120*, 500-502.
- (4) Richter, T. M. M.; Niewa, R. Chemistry of Ammonothermal Synthesis. *Inorganics* **2014**, *2*, 29-78.
- (5) Schlieper, T.; Schnick, W. Hochtemperatur-Synthese und Kristallstruktur von $\text{Ca}_2\text{Si}_5\text{N}_8$. *Z. Anorg. Allg. Chem.* **1995**, *621*, 1037-1041.
- (6) Huppertz, H.; Schnick, W. Nitridosilicates - A Significant Extension of Silicate Chemistry. *Chem. Eur. J.* **1997**, *3*, 679-683.
- (7) Durach, D.; Schnick, W. Non-Condensed (Oxo)Nitridosilicates: $\text{La}_3[\text{SiN}_4]\text{F}$ and the Polymorph $\text{o-La}_3[\text{SiN}_3\text{O}]\text{O}$. *Eur. J. Inorg. Chem.* **2015**, 4095-4100.
- (8) Woike, M.; Jeitschko, W. Preparation and Crystal Structure of the Nitridosilicates $\text{Ln}_3\text{Si}_6\text{N}_{11}$ ($\text{Ln} = \text{La}, \text{Ce}, \text{Pr}, \text{Nd}, \text{Sm}$) and LnSi_3N_5 ($\text{Ln} = \text{Ce}, \text{Pr}, \text{Nd}$). *Inorg. Chem.* **1995**, *34*, 5105-5108.
- (9) Zeuner, M.; Pagano, S.; Schnick, W. Nitridosilicates and Oxonitridosilicates: From Ceramic Materials to Structural and Functional Diversity. *Angew. Chem.* **2011**, *123*, 7898-7920; *Angew. Chem. Int. Ed.* **2011**, *50*, 7754-7775.
- (10) Kubus, M.; Meyer, H.-J. A Low-Temperature Synthesis Route for CaAlSiN_3 Doped with Eu^{2+} . *Z. Anorg. Allg. Chem.* **2013**, *639*, 669-671.
- (11) Pust, P.; Wochnik, A. S.; Baumann, E.; Schmidt, P. J.; Wiechert, D.; Scheu, C.; Schnick, W. $\text{Ca}[\text{LiAl}_3\text{N}_4]:\text{Eu}^{2+}$ - A Narrow-Band Red-Emitting Nitridolithoaluminate. *Chem. Mater.* **2014**, *26*, 3544-3549.
- (12) Schmiechen, S.; Nietschke, F.; Schnick, W. Structural Relationship between the Mg-containing Nitridosilicates $\text{Ca}_2\text{Mg}[\text{Li}_2\text{Si}_2\text{N}_6]$ and $\text{Li}_2\text{Ca}_2[\text{Mg}_2\text{Si}_2\text{N}_6]$. *Eur. J. Inorg. Chem.* **2015**, 1592-1597.
- (13) Strobel, P.; Schmiechen, S.; Siegert, M.; Tücks, A.; Schmidt, P. J.; Schnick, W. Narrow-Band Green Emitting Nitridolithosilicate $\text{Ba}[\text{Li}_2(\text{Al}_2\text{Si}_2)\text{N}_6]:\text{Eu}^{2+}$ with Framework Topology *whj* for LED/LCD Backlight Applications. *Chem. Mater.* **2015**, *27*, 6109-6115.
- (14) Poesl, C.; Neudert, L.; Schnick, W. Layered Nitridomagnesosilicates $\text{CaMg}_2\text{GaN}_3$ and $\text{CaMg}_2\text{Ga}_2\text{N}_4$. *Chem. Eur. J.* **2017**, 1067-1074.
- (15) Meyer, H.-J. Solid state metathesis reactions as a conceptional tool in the synthesis of new materials. *Dalton Trans.* **2010**, *39*, 5973-5982.
- (16) Schmiechen, S.; Schneider, H.; Wagatha, P.; Hecht, C.; Schmidt, P. J.; Schnick, W. Towards New Phosphors for Application in Illumination-Grade White pc-LEDs: The Nitridomagnesosilicates $\text{Ca}[\text{Mg}_3\text{SiN}_4]:\text{Ce}^{3+}$, $\text{Sr}[\text{Mg}_3\text{SiN}_4]:\text{Eu}^{2+}$, and $\text{Eu}[\text{Mg}_3\text{SiN}_4]$. *Chem. Mater.* **2014**, *26*, 2712-2719.
- (17) Schmiechen, S.; Strobel, P.; Hecht, C.; Reith, T.; Siegert, M.; Schmidt, P. J.; Huppertz, P.; Wiechert, D.; Schnick, W. Nitridomagnesosilicate $\text{Ba}[\text{Mg}_3\text{SiN}_4]:\text{Eu}^{2+}$ and Structure-Property Relations of Similar Narrow-Band Red Nitride Phosphors. *Chem. Mater.* **2015**, *27*, 1780-1785.
- (18) Takeda, T.; Hirosaki, N.; Funahashi, S.; Xie, R.-J. Narrow-Band Green-Emitting Phosphor $\text{Ba}_2\text{LiSi}_7\text{AlN}_{12}:\text{Eu}^{2+}$ with High Thermal Stability Discovered by a Single Particle Diagnosis Approach. *Chem. Mater.* **2015**, *27*, 5892-5898.
- (19) Uheda, K.; Hirosaki, N.; Yamamoto, H. Host lattice materials in the system $\text{Ca}_3\text{N}_2 - \text{AlN} - \text{Si}_3\text{N}_4$ for white light emitting diode. *Phys. Status Solidi A* **2006**, *203*, 2712-2717.
- (20) Park, D. G.; Dong, Y.; DiSalvo, F. J. $\text{Sr}(\text{Mg}_2\text{Ge})\text{N}_4$ and $\text{Sr}(\text{Mg}_2\text{Ga})\text{N}_4$: New isostructural Mg-containing quaternary nitrides with nitridometallate anions of $[(\text{Mg}_2\text{Ge})\text{N}_4]^{2-}$ and $[(\text{Mg}_2\text{Ga})\text{N}_4]^{2-}$ in a 3D-network structure. *Solid State Sci.* **2008**, *10*, 1846-1852.
- (21) Pust, P.; Hintze, F.; Hecht, C.; Weiler, V.; Locher, A.; Zitnanska, D.; Harm, S.; Wiechert, D.; Schmidt, P. J.; Schnick, W. Group (III) Nitrides $\text{M}[\text{Mg}_2\text{Al}_2\text{N}_4]$ ($\text{M} = \text{Ca}, \text{Sr}, \text{Ba}, \text{Eu}$) and $\text{Ba}[\text{Mg}_2\text{Ga}_2\text{N}_4]$ - Structural Relation and Nontypical Luminescence Properties of Eu^{2+} Doped Samples. *Chem. Mater.* **2014**, *26*, 6113-6119.
- (22) Yamane, H.; Kikkawa, S.; Koizumi, M. Preparation of Lithium Silicon Nitrides and their Lithium Ion Conductivity. *Solid State Ionics* **1987**, *25*, 183-191.
- (23) Bhambra, M. S.; Fray, D. J. The Electrochemical Properties of Li_3AlN_2 and Li_2SiN_2 . *J. Mater. Sci.* **1995**, *30*, 5381-5388.
- (24) Ziegler, A.; Idrobo, J. C.; Cinibulk, M. K.; Kisiowski, C.; Browning, N. D.; Ritchie, R. O. Interface Structure and Atomic Bonding Characteristics in Silicon Nitride Ceramics. *Science* **2004**, *306*, 1768-1770.
- (25) Jack, K. H. Sialons and Related Nitrogen Ceramics. *J. Mater. Sci.* **1976**, *11*, 1135-1158.
- (26) Yamane, H.; Kikkawa, S.; Koizumi, M. Preparation and electrochemical properties of double-metal nitrides containing lithium. *J. Power Sources* **1987**, *20*, 311-315.
- (27) Durach, D.; Neudert, L.; Schmidt, P. J.; Oeckler, O.; Schnick, W. $\text{La}_3\text{BaSi}_5\text{N}_{10}\text{O}_2:\text{Ce}^{3+}$ - A Yellow Phosphor with an Unprecedented Tetrahedra Network Structure Investigated by Combination of Electron Microscopy and Synchrotron X-ray Diffraction. *Chem. Mater.* **2015**, *27*, 4832-4838.
- (28) Wang, L.; Zhang, H.; Wang, X.-J.; Dierre, B.; Suehiro, T.; Takeda, T.; Hirosaki, N.; R.-J. Xie Europium(II)-activated oxonitridosilicate yellow phosphor with excellent quantum efficiency and thermal stability - a robust spectral conversion material for highly efficient and reliable white LEDs. *Phys. Chem. Chem. Phys.* **2015**, *17*, 15797-15804.
- (29) Höppe, H. A.; Lutz, H.; Morys, P.; Schnick, W.; Seilmeier, A. Luminescence in Eu^{2+} -doped $\text{Ba}_2\text{Si}_5\text{N}_8$: fluorescence, thermoluminescence, and upconversion. *J. Phys. Chem. Solids* **2000**, *61*, 2001-2006.
- (30) Mueller-Mach, R.; Mueller, G.; Krames, M. R.; Höppe, H. A.; Stadler, F.; Schnick, W.; Juestel, T.; Schmidt, P. J. Highly efficient all-nitride phosphor-converted white light emitting diode. *Phys. Status Solidi A* **2005**, *202*, 1727-1732.
- (31) Zeuner, M.; Schmidt, P. J.; Schnick, W. One-Pot Synthesis of Single-Source Precursors for nanocrystalline LED

Phosphors $M_2Si_5N_8:Eu^{2+}$ ($M = Sr, Ba$). *Chem. Mater.* **2009**, *21*, 2467-2473.

(32) Schnick, W. Shine a light with nitrides. *Phys. Status Solidi RRL* **2009**, *3*, A113-A114.

(33) Xie, R.-J.; Hirotsaki, N.; Takeda, T.; Suehiro, T. On the Performance Enhancement of Nitride Phosphors as Spectral Conversion Materials in Solid State Lighting. *ECS J. Solid State Sci. Technol.* **2013**, *2*, R3131-R3040.

(34) Pust, P.; Weiler, V.; Hecht, C.; Tücks, A.; Wochnik, A. S.; Henß, A.-K.; Wiechert, D.; Scheu, C.; Schmidt, P. J.; Schnick, W. Narrow-band red-emitting $Sr[LiAl_3N_4]:Eu^{2+}$ as a next-generation LED-phosphor material. *Nat. Mater.* **2014**, *13*, 891-896.

(35) Krames, M.; Müller, G. O.; Mueller-Mach, R.; Bechtel, H.-H.; Schmidt, P. J., Wavelength conversion for producing white light from a high power blue light emitting diode (LED). *PCT Int. Appl. WO2010131333 A1*, **2010**.

(36) Brokamp, T. Darstellung und Charakterisierung einiger ternärer Tantalnitride mit Lithium, Magnesium oder Calcium. Thesis, Universität Dortmund, **1991**.

(37) Sheldrick, G. M. *SHELXS-97: A program for crystal structure solution*, University of Göttingen, 1997.

(38) Sheldrick, G. M. A short history of SHELX. *Acta Crystallogr., Sect. A: Found. Crystallogr.* **2008**, *64*, 112-122.

(39) Sheldrick, G. M. *SHELXL-97: A program for structure refinement*, University of Göttingen, 1997.

(40) Liebau, F. *Structural Chemistry of Silicates*, Springer, Berlin, **1986**. (The terms *dreier* ring, *vierer* ring, *sechser* ring and *achter* ring was coined by Liebau and is derived from the German words *drei* = 3, *vier* = 4, *sechs* = 6 and *acht* = 8. A dreier ring comprises three tetrahedra centers.)

(41) Pagano, S.; Lupart, S.; Zeuner, M.; Schnick, W. Tuning the Dimensionality of Nitridosilicates in Lithium Melts. *Angew. Chem.* **2009**, *121*, 6453-6456; *Angew. Chem. Int. Ed.* **2009**, *48*, 6335-6338.

(42) Lupart, S.; Schmichen, S.; Schnick, W. $Li_4Ca_3Si_2N_6$ and $Li_4Sr_3Si_2N_6$ - Quaternary Lithium Nitridosilicates with Isolated $[Si_2N_6]^{10-}$ Ions. *Z. Anorg. Allg. Chem.* **2010**, *636*, 1907-1909.

(43) Zeuner, M.; Pagano, S.; Hug, S.; Pust, P.; Schmichen, S.; Scheu, C.; Schnick, W. $Li_2CaSi_2N_4$ and $Li_2SrSi_2N_4$ - a Synthetic Approach to Three-Dimensional Lithium Nitridosilicates. *Eur. J. Inorg. Chem.* **2010**, 4945-4951.

(44) Lupart, S.; Pagano, S.; Oeckler, O.; Schnick, W. $Li_2Sr_4[Si_2N_5]N$ - A Layered Lithium Nitridosilicate Nitride. *Eur. J. Inorg. Chem.* **2011**, 2118-2123.

(45) Baur, W. H. Effective Ionic Radii in Nitrides. *Crystallogr. Rev.* **1987**, *1*, 59-83.

(46) Wagatha, P.; Pust, P.; Weiler, V.; Wochnik, A. S.; Schmidt, P. J.; Scheu, C.; Schnick, W. $Ca_{8.75}Li_{10.5}[Al_{39}N_{55}]:Eu^{2+}$ - Supertetrahedron Phosphor for Solid-State Lighting. *Chem. Mater.* **2016**, *28*, 1220-1226.

(47) Hübenthal, R. *MAPLE: A program for calculation of Madelung part of lattice energy*, version 4, University of Gießen, Germany, 1993.

(48) Hoppe, R. Madelung Constants. *Angew. Chem.* **1966**, *78*, 52-63; *Angew. Chem. Int. Ed.* **1966**, *5*, 95-106.

(49) Hoppe, R. The Coordination Number - an "Inorganic Chameleon". *Angew. Chem.* **1970**, *82*, 7-16; *Angew. Chem. Int. Ed.* **1970**, *9*, 25-34.

(50) Lupart, S.; Gregori, G.; Maier, J.; Schnick, W. $Li_{14}Ln_5[Si_{11}N_{19}O_5]O_2F_2$ with $Ln = Ce, Nd$ - Representatives of a Family of Potential Lithium Ion Conductors. *J. Am. Chem. Soc.* **2012**, *134*, 10132-10137.

(51) Lupart, S.; Schnick, W. $LiCa_3Si_2N_5$ - A Lithium Nitridosilicate with a $[Si_2N_5]^{7-}$ Double-Chain. *Z. Anorg. Allg. Chem.* **2012**, *638*, 2015-2019.

(52) Dorenbos, P. Anomalous luminescence of Eu^{2+} and Yb^{2+} in inorganic compounds. *J. Phys.: Condens. Matter* **2003**, *15*, 2645-2665.

(53) Lin, Y.-C.; Karlsson, M.; Bettinelli, M. Inorganic Phosphor Materials. *Top. Curr. Chem.* **2016**, *374*, 21.

(54) Braun, C.; Seibald, M.; Börger, S. L.; Oeckler, O.; Boyko, T. D.; Moewes, A.; Miehe, G.; Tücks, A.; Schnick, W. Material Properties and Structural Characterization of $M_3Si_6O_{12}N_2:Eu^{2+}$ ($M = Ba, Sr$) - A Comprehensive Study on a Promising Green Phosphor for pc-LEDs. *Chem. Eur. J.* **2010**, *16*, 9646-9657.

(55) Dorenbos, P. Energy of the first $4f^7 \rightarrow 4f^65d$ transition of Eu^{2+} in inorganic compounds. *J. Lumin.* **2003**, *104*, 239-260.

(56) Wilhelm, D.; Baumann, D.; Seibald, M.; Wurst, K.; Heymann, G.; Huppertz, H. Narrow-Band Red Emission in the Nitridolithoaluminate $Sr_4[LiAl_3N_4]:Eu^{2+}$. *Chem. Mater.* **2017**, *29*, 1204-1209.

(57) Jaffe, P. M.; Banks, E. Oxidation States of Europium in the Alkaline Earth Oxide and Sulfide Phosphors. *J. Electrochem. Soc.* **1955**, *102*, 518-523.

(58) Yamashita, N. Coexistence of the Eu^{2+} and Eu^{3+} Centers in the $CaO:Eu$ Powder Phosphor. *J. Electrochem. Soc.* **1993**, *140*, 840-843.

(59) Kunkel, N.; Kohlmann, H.; Sayede, A.; Springborg, M. Alkaline-Earth Metal Hydrides as Novel Host Lattices for Eu^{II} Luminescence. *Inorg. Chem.* **2011**, *50*, 5873-5875.

(60) Strobel, P.; Weiler, V.; Hecht, C.; Schmidt, P. J.; Schnick, W. Luminescence of the Narrow-Band Red Emitting Nitridomagnesiumsilicate $Li_2(Ca_{1-x}Sr_x)_2[Mg_2Si_2N_6]:Eu^{2+}$ ($x = 0-0.06$). *Chem. Mater.* **2017**, *29*, 1377-1383.

(61) Meijerink, A.; Blasse, G. Luminescence Properties of Eu^{2+} -Activated Alkaline Earth Haloborates. *J. Lumin.* **1989**, *43*, 283-289.

(62) Pust, P.; Schmidt, P. J.; Schnick, W. A revolution in lighting. *Nat. Mater.* **2015**, *14*, 454-458.

(63) Pattison, P. M.; Tsao, J. Y.; Krames, M. R. Light-emitting diode technology status and directions: Opportunities for horticultural lighting. *Acta Hort.* **2016**, *1134*, 413-426.

Insert Table of Contents artwork here

